PNAS
www.pnas.org

Supplementary Information for

**PTPN1/2-mediated dephosphorylation of MITA/STING promotes its 20S proteasomal degradation and attenuates innate antiviral response**

Tian Xia, Xue-Mei Yi, Xin Wu, Jun Shang and Hong-Bing Shu

Hong-Bing Shu
Email: shuh@whu.edu.cn

**This PDF file includes:**

Supplementary text
Figures S1 to S10



www.pnas.org/cgi/doi/10.1073/pnas.1906431116

## Supplementary Information Text

### SI Materials and Methods

**Reagents, antibodies, cells and viruses.** 2'3'-cGAMP and Lipofectamine 2000 (InvivoGen); polybrene (Millipore); SYBR (Bio-Rad); digitonin (Sigma); ER-Tracker™ Blue-White DPX (ThermoFisher); MG132 and 3-MA (MCE); human 20S Proteasome Protein (R&D); Dual-Specific Luciferase Assay Kit (Promega); ELISA kits for human and murine IFN-β (PBL), human IL-6 and murine CXCL10 (BOSTER) were purchased for the indicated manufacturers.

Mouse antibodies against HA (Origene), FLAG and β-actin (Sigma), GST (proteintech), PTPN1/PTP1B (Abcam); rabbit antibodies against TBK1 and phospho-TBK1 (S172) (Abcam), MITA/STING, phospho-MITA/STING (S366) and phospho-IRF3 (S396) (CST), and PTPN2 (proteintech) were purchased for the indicated manufacturers.

HEK293 and THP1 cells were purchased from ATCC. *Mita*$^{-/-}$ MLFs , HSV-1 and SeV were previously describe (1).

**Constructs.** Expression plasmids for FLAG-, RFP-, or GPF tagged PTPN1, PTPN2 and their mutants, and HA-, FLAG-, Cherry-, or GST-tagged MITA and its mutants were constructed by standard molecular biology techniques. HA-tagged cGAS, MITA, TBK1 and IRF3 were previously described (2).

***Ptpn1* knockout mice and genotyping.** *Ptpn1* gene-knockout mice with a C57/B6 background were generated utilizing the CRISPR/Cas9 system by Nanjing Biomedical Research Institute of Nanjing University (NBRI). *Ptpn1* gene has 9 exons, with the ATG start codon in exon 1 and TGA stop codon in exon 9. Intron 1-2 and intron 8-9 of *Ptpn1* were respectively targeted by specific gRNAs, which directed Cas9 endonuclease cleavage of the *Ptpn1* gene resulting in a double-strand break (DSB). Such breaks would be repaired by non-homologous end joining (NHEJ), and result in the disruption of *Ptpn1*.

Genotyping by PCR was performed using the following pairs of primers: WT (F): 5′-CACCTTGGTGAGGAGTCCTGTG -3′; WT (R): 5′- GAGGCATTCTGGCACACAGC -3′; KO (F): 5′- TGAGATGAAGGAAGGCAGGG -3′; KO (R): 5′-AGAATGAGGGCAGCCAGGCTAC -3′. Amplification of the WT allele with primers WT (F) and WT (R) generates a 466-bp fragment, whereas amplification of the disrupted allele with primers KO (F) and KO (R) generates a 785-bp fragment.

***Ptpn2* knockout mice and genotyping.** *Ptpn2* gene-knockout mice with a C57/B6 background were generated utilizing the CRISPR/Cas9 system by Nanjing Biomedical Research Institute of Nanjing University (NBRI). *Ptpn2* gene has 9 exons, with the ATG start codon in exon 1 and TGA stop codon in exon 9. Intron 1-2 and intron 2-3 of *Ptpn2* were respectively targeted by specific gRNAs, which directed Cas9 endonuclease cleavage of the *Ptpn2* gene resulting in a double-strand break (DSB). Such breaks would be repaired by non-homologous end joining (NHEJ). This led to frame shift mutation from exon 3 of *ptpn2* and an early stop codon.

Genotyping by PCR was performed using the following pairs of primers: WT (F): 5′-TAGTAGGAGTGGGATTGAGAGC -3′; WT (R): 5′-GCTAACAGTTTCATCTGAGTAATC -3′; KO (R): 5′-GGAAATGCTGAGCTGTTATAGG -3′. Amplification of the WT allele with primers WT (F) and WT (R) generates a 564-bp fragment, whereas amplification of the disrupted allele with primers WT (F) and KO (R) generates a 720-bp fragment.

**DNA Oligonucleotides.** The following oligonucleotides were used to stimulate cells: ISD45: 5'-TACAGATCTACTAGTGATCTATGACTGATCTGTACATGATCTACA-3'; dsDNA90: 5'-TACAGATCTACTAGTGATCTATGACTGATCTGTACATGATCTACATACAGA TCTACTAGTGATCTATGACTGATCTGTACATGATCTACA-3'; HSV120: 5'-AGACGGTATATTTTTGCGTTATCACTGTCCCGGATTGGACACGGTCTTGT GGGATAGGCATGCCCAGAAGGCATATTGGGTTAACCCCTTTTTATTTGTGGCG GGTTTTTTGGAGGACTT-3'.

**Transfection and reporter assays.** HEK293 cells were transfected by standard calcium phosphate precipitation method. MLFs were transfected by Lipofectamine 2000 according to procedures recommended by the manufacturer. Luciferase assays were performed using a Dual-Specific Luciferase Assay Kit. To normalize for transfection efficiency, pRL-TK (*Renilla* luciferase) reporter plasmid (0.01 μg) was added to each transfection. Firefly luciferase activities were normalized on the basis of *Renilla* luciferase activities.

**qPCR.** Total RNA was isolated for qPCR analysis to measure mRNA abundance of the indicated genes. Data shown are the relative abundance of the indicated mRNA derived from human or mouse cells normalized to that of GAPDH. Gene-specific primer sequences were as followed**:**
*GAPDH:* GACAAGCTTCCCGTTCTCAG, GAGTCAACGGATTTGGTGGT;
*IFNB1:* TTGTTGAGAACCTCCTGGCT, TGACTATGGTCCAGGCACAG;
*IFNA4:* GTTCCAGAAGGCTCAAGCCATC, TAGGAGGCTCTGTTCCCAAGCA;
*CXCL10:* GGTGAGAAGAGATGTCTGAATCC, GTCCATCCTTGGAAGCACTGCA;
*ISG56:* TCATCAGGTCAAGGATAGTC, CCACACTGTATTTGGTGTCTACG;
*IL6:* GCCGCATCGCCGTCTCCTAC, CCTCAGCCCCCTCTGGGGTC;
*TNFA:* GCCGCATCGCCGTCTCCTAC, CCTCAGCCCCCTCTGGGGTC;
*IKBA:* CGGGCTGAAGAAGGAGCGGC, ACGAGTCCCCGTCCTCGGTG;
*Gapdh*: ACGGCCGCATCTTCTTGTGCA, ACGGCCAAATCCGTTCACACC;
*Ifnb1:* TCCTGCTGTGCTTCTCCACCACA, AAGTCCGCCCTGTAGGTGAGGTT
*Isg56*: ACAGCAACCATGGGAGAGAATGCTG,
ACGTAGGCCAGGAGGTTGTGCAT;
*Cxcl10*: ATCATCCCTGCGAGCCTATCCT, GACCTTTTTTGGCTAAACGCTTTC;
*Il-6:* TCTGCAAGAGACTTCCATCCAGTTGC, AGCCTCCGACTTGTGAAGTGGT.

**CRISPR-Cas9 knockout.** The protocols for genome engineering using the CRISPR-Cas9 system were previously described (3, 4). Briefly, double-stranded oligonucleotides

corresponding to the target sequences were cloned into the lenti-CRISPR-V2 vector, which was cotransfected with packaging plasmids into HEK293 cells. Two days after transfection, the viruses were harvested and used to infect THP1 or MLF cells. The infected cells were selected with puromycin (1 μg/ml) for at least 5 days.
The following gRNA sequences were used. Human PTPN1: 5'-GTACAGTGCGACAGCTAGAAT-3'; Human PTPN2: 5'-GCACTACAGTGGATCACCGC-3'.

**Affinity purification.** THP-1 cells were mock-infected or infected with HSV-1 for 8 h. The cells were harvested by centrifugation at 1000 × g for 3 min and lysed with 1 ml lysis buffer (50 mM Tris-HCl [pH 7.4], 150 mM NaCl, 1% NP40, complete protease inhibitor mixture) at 4°C for 1 h. Lysates were cleared by centrifugation (4000 × g) at 4°C for 20 min. The supernatants were mixed with anti-MITA monoclonal antibody (2 μg) and protein G magnetic beads (50 μl) and then incubated at 4°C for 4 h. The beads were washed three times with washing buffer (150 mM NaCl, 50 mM Tris-HCl [pH 7.5]).

**Confocal microscopy.** HEK293 or MLF cells were transfected with the indicated plasmids by Lipo2000. After transfection for 20 h, the cells were fixed with 4% paraformaldehyde for 15-20 min and then washed with PBS for 3 times. The nuclei were stained with DAPI for 2 min and then washed with PBS for 3 times. Imaging of the cells was carried out using Zeiss LSM880 confocal microscope under a 60X oil objective.

**Coimmunoprecipitation and immunoblotting analysis.** Cells were lysed in NP-40 lysis buffer (20 mM Tris-HCl [pH7.4], 150 mM NaCl, 1 mM EDTA, 1% NP-40, 10 μg/ml aprotinin, 10 μg/ml leupeptin, 1 mM phenylmethylsulfonyl fluoride). Co-immunoprecipitation and immunoblotting analysis were performed as previously described (5).

**Measurements of viral replication.** THP-1 cells ($1\times10^6$) were grown in 12-well plate and subsequent infected with HSV-1 [multiplicity of infection (MOI) = 0.01]. The supernatants were harvested 48 h later and used to infect confluent Vero cells. Plaque assays were performed as described (6).

**Measurement of cGAMP activity.** THP-1 cells ($2\times10^7$) were mock-transfected or transfected with HT-DNA (0.5 mg/ml) for 4 hr. Cells were then homogenized by dunce homogenizer in hypotonic buffer (10 mM Tris-HCl [pH 7.4], 10 mM KCl, 1.5 mM $MgCl_2$). After centrifugation at 13,000 rpm for 20 min, the supernatant was heated at 95 °C for 10 min and centrifuged at 13,000 rpm for 10 min to remove denatured proteins. The heat-resistant supernatants containing cGAMP were delivered to digitonin-permeabilized MLF at 37°C for 30 min and then cells were further cultured with regular medium for another 4 hr before qPCR analysis.

**ELISA.** THP-1 cells were infected with HSV-1 for 10 h. The culture media were collected for measurement of IFN-β and IL-6 cytokines by ELISA.

**Digitonin permeabilization.** cGAMP was delivered to MLFs pretreated with digitonin

permeabilization solution (50 mM HEPES [pH 7.0], 100 mM KCl, 3 mM $MgCl_2$, 0.1 mM DTT, 85 mM Sucrose, 0.2% BSA, 1 mM ATP, 0.1 mM GTP and 10μg/ml digitonin) at 37°C for 30 min (7).

**HSV-1 infection in mice.** Mice were infected with HSV-1 i.p. The viability of the infected mice was monitored for 12 days. The mouse sera were collected at 8 h after infection to measure cytokine production by ELISA.

**Non-reducing analysis.** Non-reducing analysis was performed as previously described (8). In brief, MLF cells were lysed on ice for 15 min in lysis buffer (10 mM PIPES-KOH [pH 7.0], 50 mM NaCl, 5 mM $MgCl_2$, 5 mM EGTA, 1% NP40, 10% glycerol, and a mixture of protease inhibitors and phosphatase inhibitors). The lysates were mixed with 5×SDS sample buffer without 2-ME. Samples were separated by electrophoresis on 10% SDS-PAGE.

**In vitro 20S proteasome assay.** For assays with E. Coli expressed recombinant proteins, the GST-MITA mutant proteins (30 nM) were incubated with 20S proteasomes (2 nM) in a reaction buffer (25 mM HEPES, 0.5 mM EDTA [pH 7.6], 0.03% SDS). Where indicated, MG132 (50 μM) was added to the reactions to inhibit proteasomal activity.

For assays with purified proteins from mammalian cells, HA-MITA and its mutant plasmids were transfected into HEK293 cells with or without Flag-SRC plasmid. The cells were harvested and lysed with NP-40 lysis buffer. Lysates were centrifuged at 13,000 rpm at 4°C for 15 min. The supernatants were mixed with anti-HA monoclonal antibody (1 μg) and protein G beads (30 μl) and then incubated at 4°C for 4 h. The first two washes were performed with NP-40 lysis buffer containing 500 mM NaCl. The third wash was performed with PBS. The last wash was performed using 20S proteasome reaction buffer. The beads were then incubated with 20S proteasomes (0.5 μg) in the reaction buffer at 37°C for the indicated times. The reactions were terminated by the addition of 5×SDS sample buffer and followed by SDS-PAGE and immunoblotting analysis.

**Statistical analysis.** Unpaired Student's t test was used for statistical analysis with Microsoft Excel and GraphPad Prism Software. For the mouse survival study, Kaplan-Meier survival curves were generated and analyzed by Log-Rank test.

## References


1. Li Y, *et al.* (2012) LSm14A is a processing body-associated sensor of viral nucleic acids that initiates cellular antiviral response in the early phase of viral infection. *Proc Natl Acad Sci U S A* 109(29):11770-11775.
2. Lian H, *et al.* (2018) ZCCHC3 is a co-sensor of cGAS for dsDNA recognition in innate immune response. *Nat Commun* 9(1):3349.
3. Sanjana NE, Shalem O, & Zhang F (2014) Improved vectors and genome-wide libraries for CRISPR screening. *Nature methods* 11(8):783-784.
4. Shalem O, *et al.* (2014) Genome-scale CRISPR-Cas9 knockout screening in human cells. *Science* 343(6166):84-87.
5. Yan BR, *et al.* (2017) PKACs attenuate innate antiviral response by phosphorylating VISA and priming it for MARCH5-mediated degradation. *PLoS Pathog* 13(9):e1006648.
6. Lei CQ, *et al.* (2013) FoxO1 negatively regulates cellular antiviral response by promoting degradation of IRF3. *J Biol Chem* 288(18):12596-12604.
7. Liu TT, *et al.* (2016) LSm14A Plays a Critical Role in Antiviral Immune Responses by Regulating MITA Level in a Cell-Specific Manner. *J Immunol* 196(12):5101-5111.
8. Motani K, Ito S, & Nagata S (2015) DNA-Mediated Cyclic GMP-AMP Synthase-Dependent and -Independent Regulation of Innate Immune Responses. *J Immunol* 194(10):4914-4923.

A

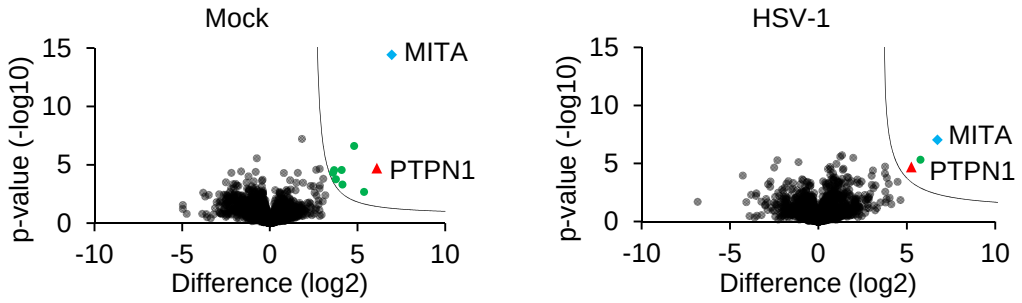


B

High-confidence interactors of MITA

| Gene | Mock | | HSV-1 8h | | Score | MS/MS count |
|---|---|---|---|---|---|---|
| | Ratio | P-value | Ratio | P-value | | |
| MITA* | 6.952 | 3.85E-15 | 6.724 | 9.23E-08 | 323.310 | 430 |
| PTPN1* | 6.099 | 1.92E-05 | 5.255 | 1.94E-05 | 185.090 | 71 |
| INT1 | 4.090 | 2.84E-05 | 4.024 | 9.00E-03 | 64.940 | 36 |
| SURF4 | 4.136 | 4.92E-04 | 0.945 | 6.47E-02 | 42.350 | 13 |
| MITD1 | 3.598 | 4.75E-05 | 0.413 | 6.25E-01 | 13.745 | 6 |
| RBM45 | 3.759 | 1.75E-04 | 3.015 | 6.86E-04 | 11.203 | 10 |
| INT7* | 4.806 | 2.47E-07 | 5.771 | 4.66E-06 | 11.068 | 13 |
| EI2BB | 5.370 | 2.10E-03 | 3.207 | 1.06E-01 | 10.354 | 7 |
| KPCD2 | 3.664 | 2.94E-05 | 2.864 | 7.52E-03 | 6.793 | 4 |

C

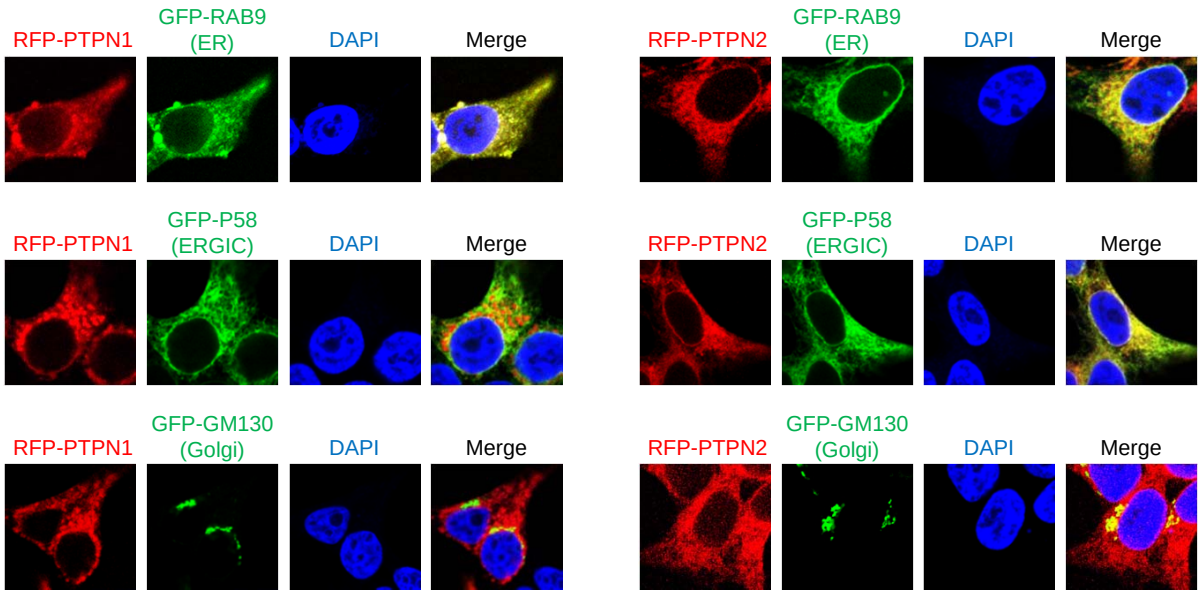


**Fig. S1. PTPN1 and PTPN2 are MITA-associated proteins.**

(A) Identification of high-confidence interactors for MITA. The fold changes and p-values of the identified proteins between MITA and control pull-downs were calculated and plotted on a volcano plot. In this study, we used s0 = 2 and FDR = 0.01 to set the cut-off line. The outliner proteins were identified as potential interactors of MITA with high confidence.

(B) The identified high-confidence interactors of MITA. *, proteins detected in both mock- and HSV-1-infected group.

(C) The subcellular localization of PTPN1 and PTPN2. HEK293 cells were transfected with RFP-PTPN1/PTPN2 and GFP-tagged Rab9 (ER marker), p58 (ERGIC marker) and GM130 (Golgi marker) for 20 h before confocal microscopy.

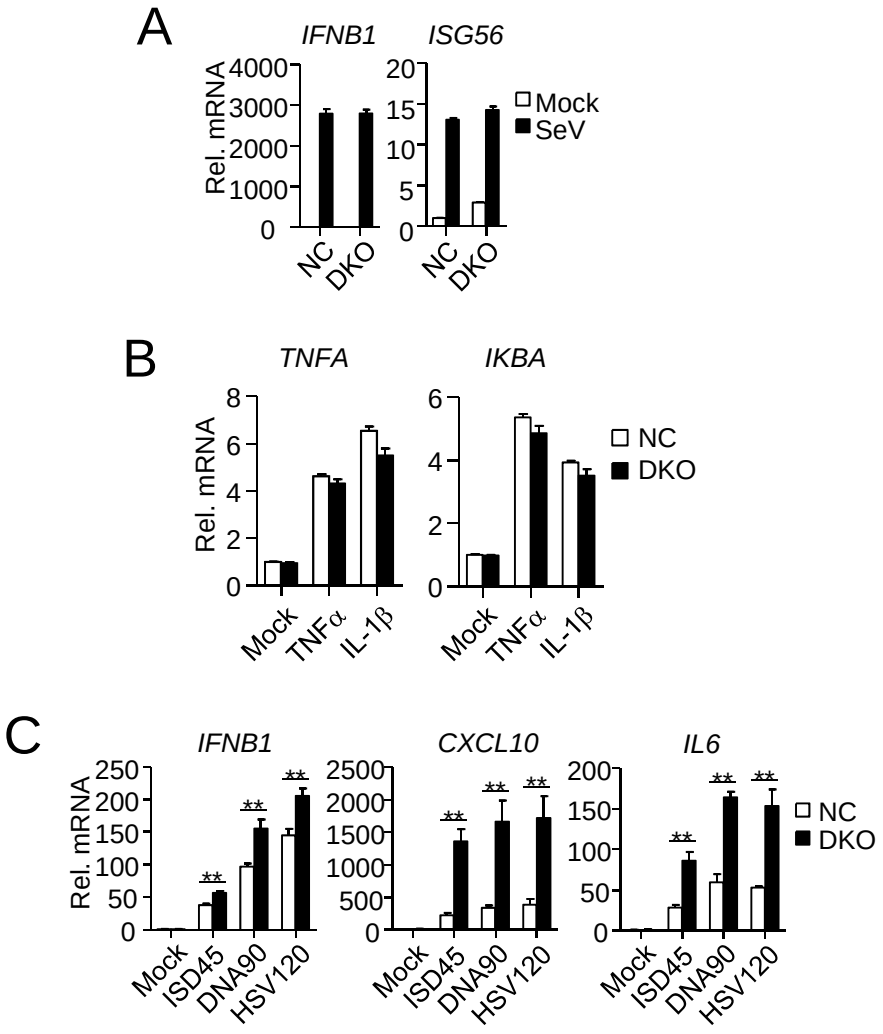


**Fig. S2. Effects of PTPN1/2 double-deficiency on transcription of downstream genes induced by various stimuli.**

(A) Effects of PTPN1/2 double-deficiency on transcription of downstream genes induced by SeV in THP-1 cells. The KO and control THP-1 cells were left un-infected or infected with SeV for 8 h before qPCR analysis.

(B) Effects of PTPN1/2-deficiency on transcription of downstream genes induced by TNFα and IL-1β.The KO and control THP-1 cells were left un-treated or treated with TNFα (10 ng/ml) or IL-1β (10 ng/ml) for 6 h before qPCR analysis.

(C) Effects of PTPN1/2 double-deficiency on transcription of downstream genes induced by cytosolic dsDNA. The DKO and control THP-1 cells were transfected with the indicated nucleic acids (3 μg/ml) for 4 h before qPCR analysis.

Graphs show mean ± SEM, n = 3. **P < 0.01.

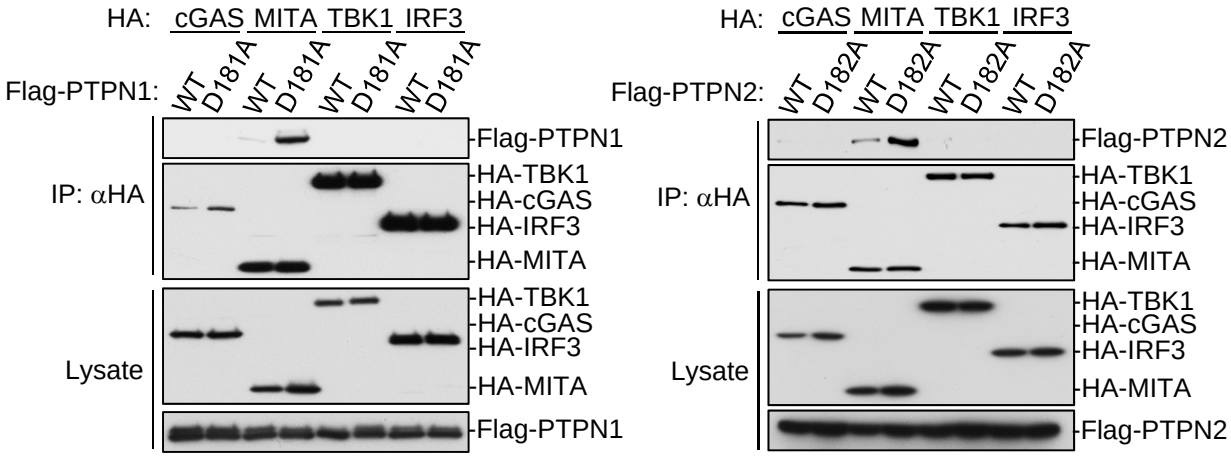


**Fig. S3. MITA interacts with "substrate-trapping" mutants of PTPN1 and PTPN2.**

HEK293 cells were transfected with the indicated plasmids for 24 h followed by co-immunoprecipitation and immunoblot analysis with the indicated antibodies.

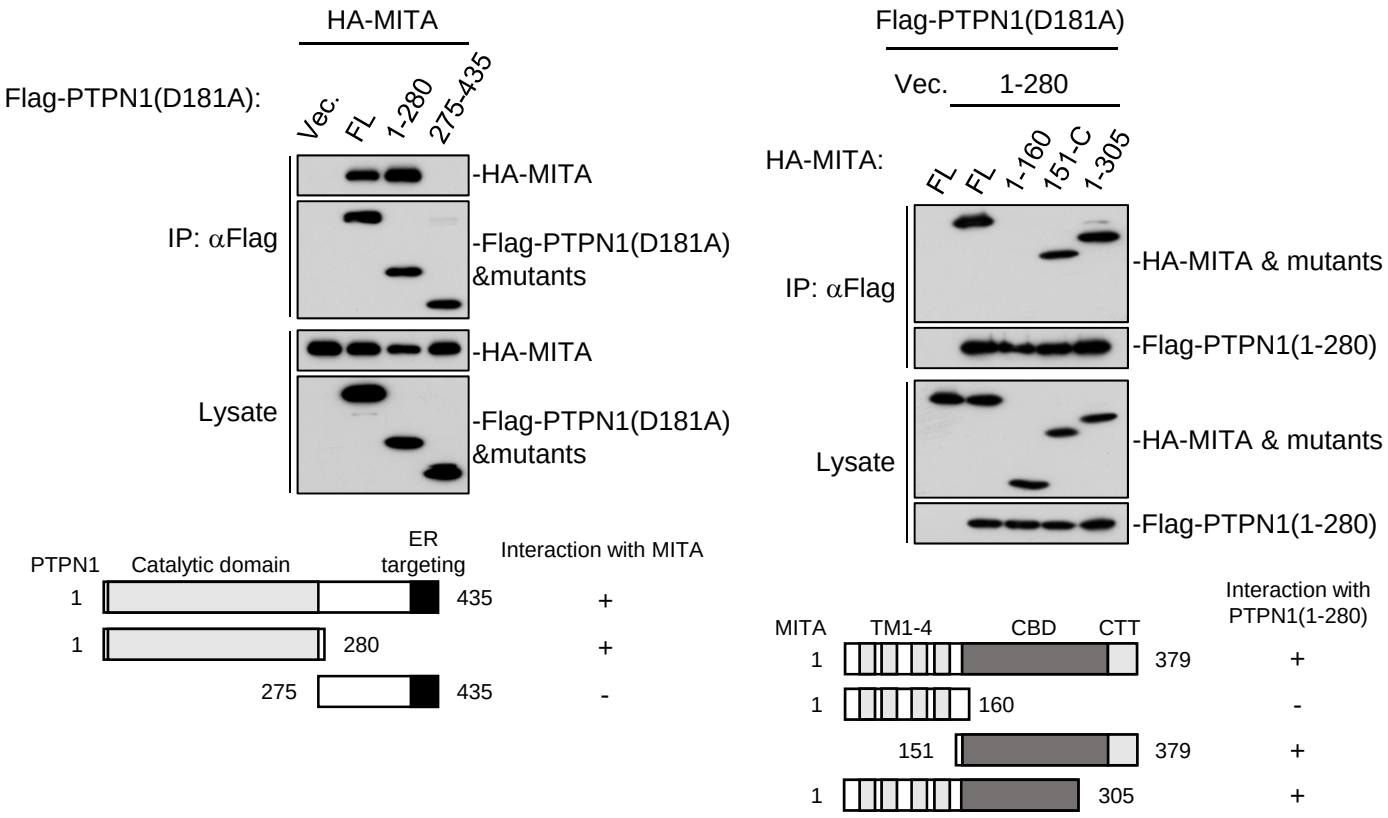


**Fig. S4. Domain mapping of the interaction between PTPN1 and MITA.**
HEK293 cells were transfected with the indicated plasmids before coimmunoprecipitation and immunoblotting analysis were performed with the indicated antibodies. -, no interaction; +, positive interaction.

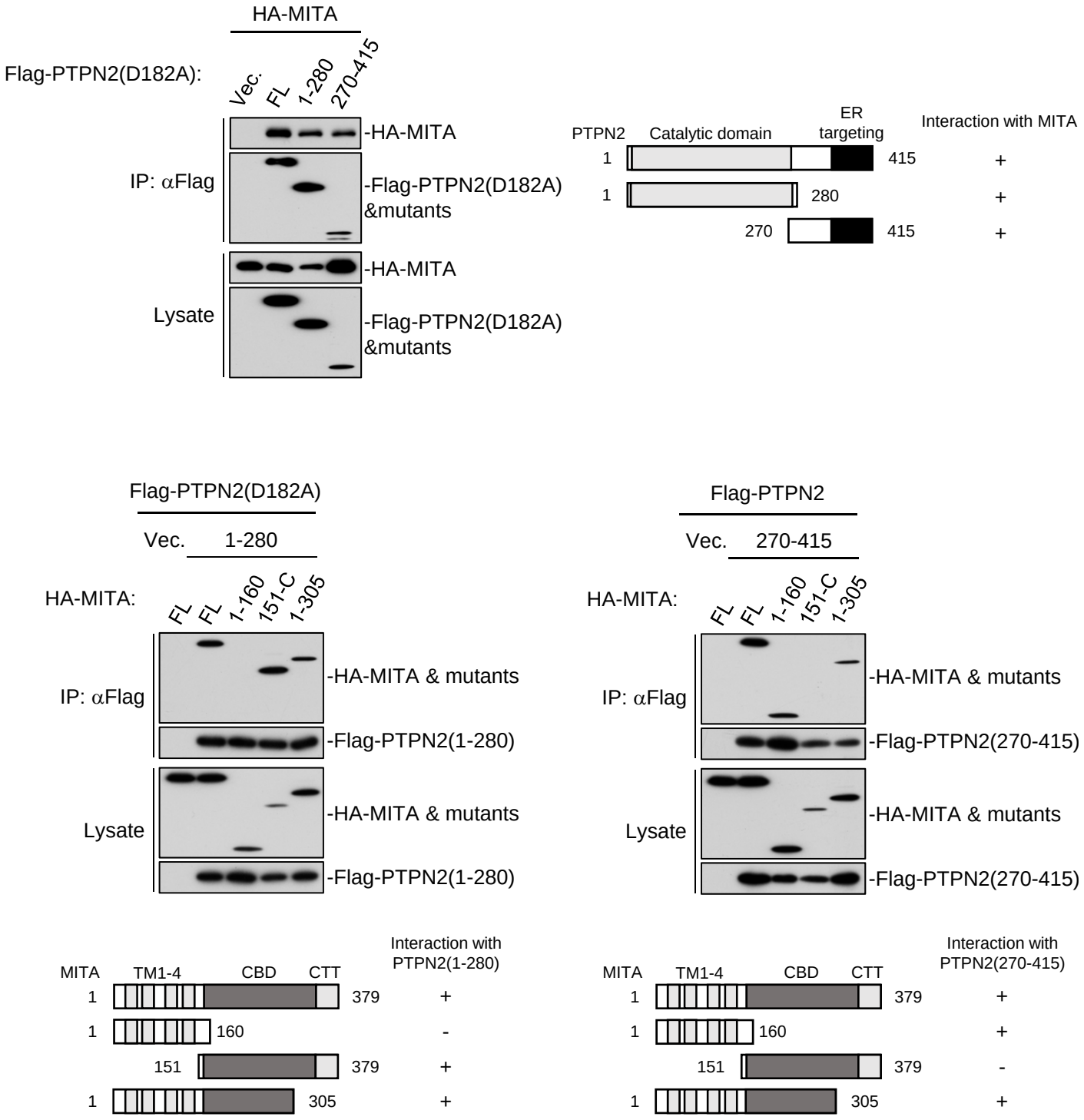


**Fig. S5. Domain mapping of the interaction between PTPN2 and MITA.**
HEK293 cells were transfected with the indicated plasmids before coimmunoprecipitation and immunoblotting analysis were performed with the indicated antibodies. -, no interaction; +, positive interaction.

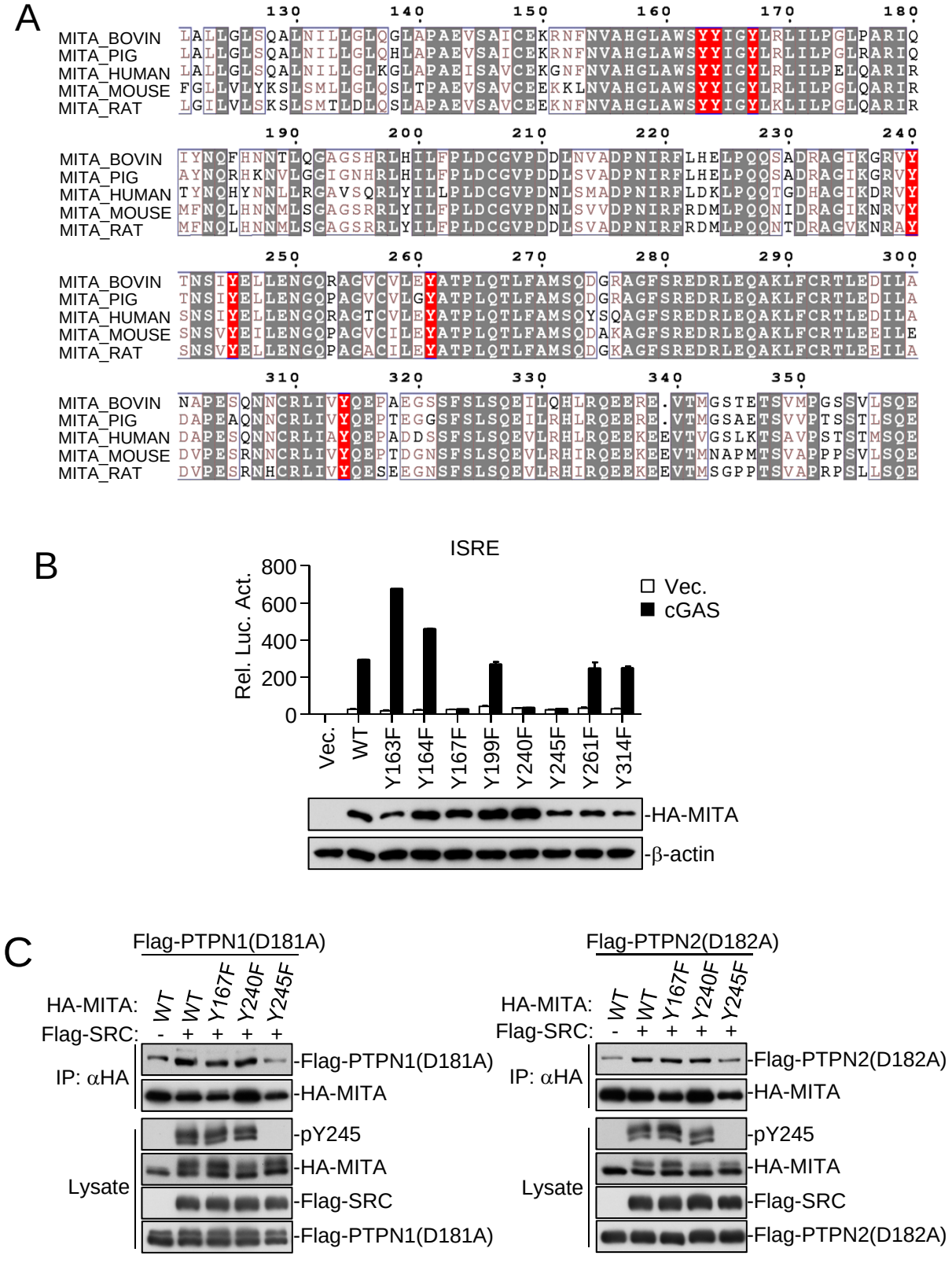


**Fig. S6. Identification of residues in the activation of MITA.**

(A) Sequence alignment of MITA from the indicated species. The sequences are corresponding to aa120-360 of human MITA. The conserved tyrosine residues are highlighted.

(B) Effects of ISRE activation mediated by MITA and its mutants. HEK293 cells were transfected with the indicated plasmids for 20 h before reporter assays and immunoblotting analysis.

(C) The interactions between PTPN1/2 substrate-trapping mutants and MITA or MITA mutants. HEK293T cells were transfected with the indicated plasmids for 24 h followed by co-immunoprecipitation and immunoblotting analysis with the indicated antibodies.

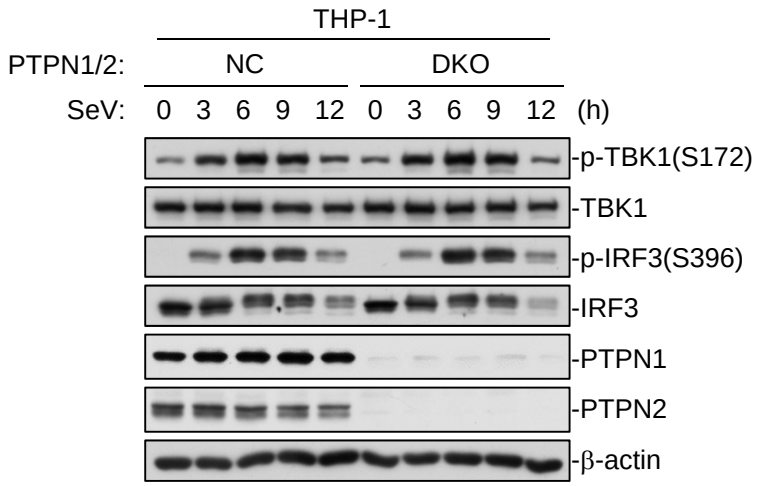


**Fig. S7. Effects of PTPN1/2-deficiency on SeV-induced signaling**
THP-1 cells were infected with SeV for the indicated times. Cell lysates were subjected to immunoblotting analysis with the indicated antibodies.

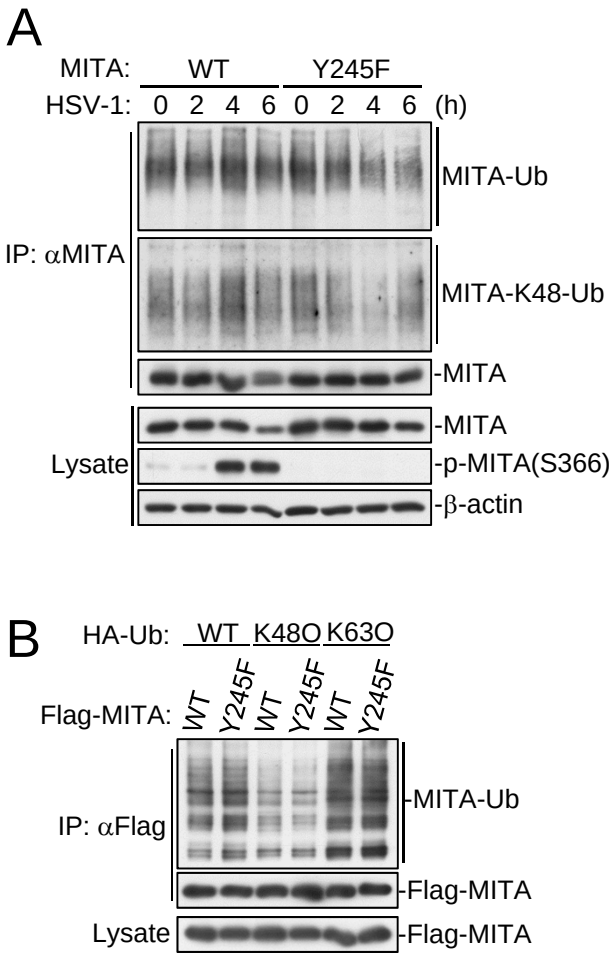


**Fig. S8. Effects of mutation of MITA Y245 on its polyubiquitination.**
(A) Mutation of MITA Y245 does not affect its K48-linked polyubiquitination of MITA. HEK293 cells were transfected with the indicated plasmids for 20 h, and then treated with MG132 (100 μM) for 6 h before coimmunoprecipitation and immunoblotting analysis. (B) Mutation of MITA Y245 does not affect HSV-1-induced K48-linked polyubiquitination of MITA. *Mita*$^{-/-}$ MLF cells reconstituted with MITA or MITA(Y245F) were treated with MG132 for 1 h, then infected with HSV-1 (MOI = 4) for the indicated times before coimmunoprecipitation and immunoblotting analysis.

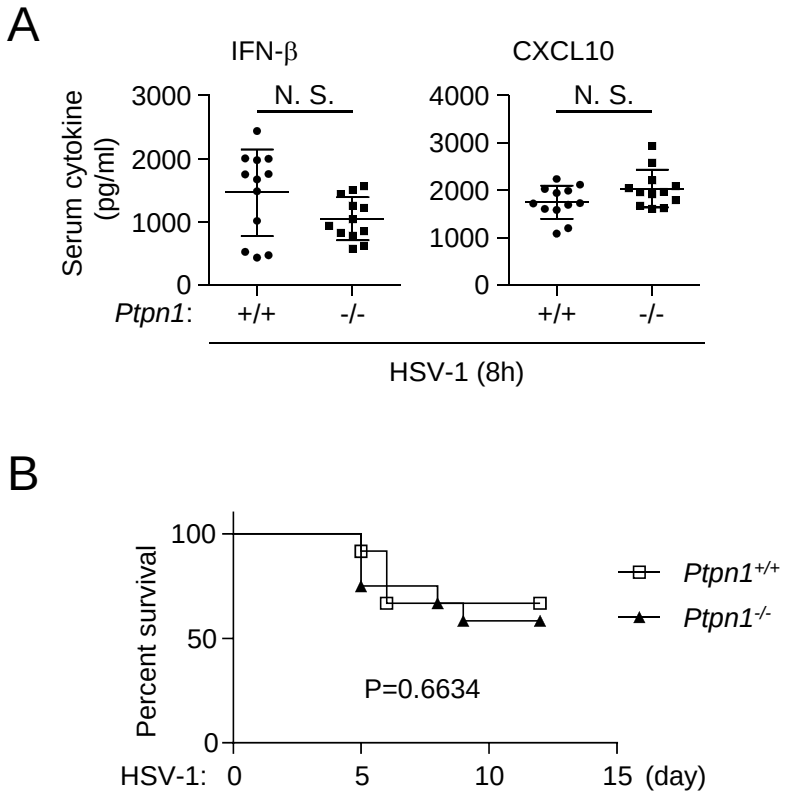


**Fig. S9. Effects of PTPN1-deficiency on host defense against HSV-1 infection in mice**

(A) *Ptpn1*$^{+/+}$ and *Ptpn1*$^{-/-}$ mice (n = 12) were infected intraperitoneally (i.p.) with HSV-1 at 5 x $10^7$ pfu per mouse for 8 h before serum cytokines were measured by ELISA.

(B) *Ptpn1*$^{+/+}$ and *Ptpn1*$^{-/-}$ mice (n = 12) were infected intraperitoneally (i.p.) with HSV-1 at 5 x $10^7$ pfu per mouse, and the survivals of mice were recorded daily for 12 days.

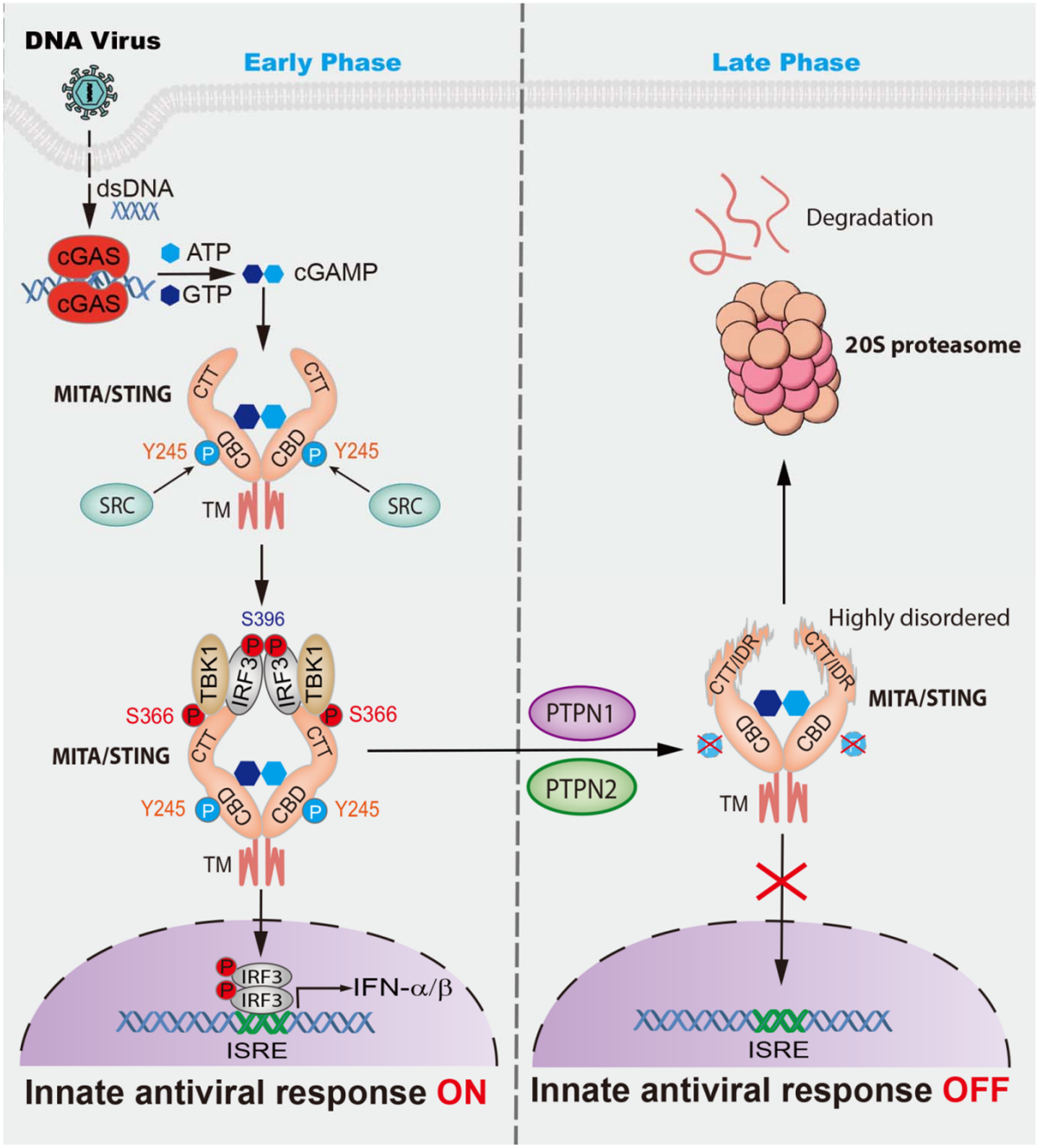


**Fig. S10. A schematic presentation for the roles of PTPN1/2 in regulating MITA/STING-mediated innate antiviral response.**

Following DNA virus infection, cGAS recognizes viral DNA and synthesizes cGAMP. cGAMP binds to MITA/STING and induces its oligomerization and translocation from the ER to perinuclear punctate structures. The tyrosine kinase SRC phosphorylates MITA at Y245 which promotes these processes. During these processes, MITA recruits the kinase TBK1 and transcription factor IRF3. TBK1 firstly phosphorylates MITA at S366, which is important for subsequent phosphorylation of IRF3 at S399 by TBK1. This results in IRF3 activation and induction of downstream antiviral genes such as type I IFNs, leading to innate antiviral response. At the late phase of infection, the protein tyrosine phosphatases PTPN1 and PTPN2 are recruited to MITA to dephosphorylate it at Y245. This causes exposure of the C-terminal intrinsically disordered region of MITA and its recogniztion by 20S proteasomes, leading to degradation of MITA and attenuation of innate antiviral response. CBD, cGAMP-binding domain; CTT, C-terminal tail; ISRE, interferon stimulating response element; TM, transmembrane domain; IDR, intrinsically disordered region.